

PHASE COMPOSITION OF PROTON-EXCHANGED WAVEGUIDES IN LiNbO₃: A SPECTROSCOPIC STUDY

M. Kuneva^{*}, S. Tonchev, E. Thatsi^a, D. Lampakis^a

Institute of Solid State Physics – Bulgarian Academy of Sciences, 72 Tzarigradsko Chaussee Blvd, 1784 Sofia, Bulgaria

^aDepartment of Physics, National Technical University of Athens, Zografou Campus Heroon Polytechniou 9, GR 15780 Athens, Greece

Waveguiding layers in LiNbO₃ crystal substrates with different crystallographic orientations were obtained using proton exchange technology. The phase composition of the waveguides was investigated by Raman, infrared and waveguide mode spectroscopy, and conclusions were made about the phases existing in the layers. The results obtained could be used for the estimation of the phase composition, and therefore of the optical and electro-optical properties of proton exchanged waveguides in LiNbO₃.

(Received December 9, 2004; accepted January 26, 2005)

Keywords: Optical waveguides, Proton exchange, IR-spectroscopy, Raman-spectroscopy

1. Introduction

The easy and fast creation of optical waveguides in the electro-optical crystal LiNbO₃, by proton exchange (PE) [1], has motivated attempts to adjust the technology for producing high quality waveguides. The hydrogen-modified diffusion surface layer has a large extraordinary refractive index change (Δn_e) and, thus, strong waveguiding and polarizing effects. The Li_{1-x}H_xNbO₃ layer formed by Li-H ion exchange shows complex phase behavior, dependant on the hydrogen concentration (value of x) [2].

Recently, attempts were made to control the phase status of the waveguide layers, by the use of new proton sources or modifications of the technological regimes. This is why the means permitting the analysis of the phase content of such layers are also strongly investigated.

2. Experiment and results

Five samples of different crystallographic orientation: Z-1, NMZ-1, NMZ-5 (Z-cut), X-3 (X-cut) and Y-2 (Y-cut) were used for the experiment. Proton exchange was performed using the technological regimes described in Table 1. Two different modifications of the PE process were used – PE in new melts (LiHSO₄, NH₄HSO₄) [3] and low-temperature PE in vapors [4].

A mode spectroscopy study was performed using the two-prism coupling [5] of a He-Ne laser ($\lambda=632.8$ nm). The IWKB method [6] was used to determine Δn_e and the depth of the waveguide layers. In the case of single-mode waveguides (LX-3, NMZ-5), mode-spectra measurements were performed in both air and water and the optical profile was reconstructed by solving the two mode-propagation equations for a step-like optical profile. The optical losses (Table 2) for each propagating mode were estimated as the ratio of input to output intensities. The infrared (IR) spectra of protonated and as-grown samples were recorded in the frequency range

* Corresponding author: kuneva@issp.bas.bg

2700-3700 cm^{-1} of the OH-stretching modes, with a Bruker LFS-113 V FTIR spectrometer, and a Gaussian-Lorentzian decomposition procedure was performed. The results are shown in Fig.1.

The micro-Raman (Ra) spectra were collected using a Jobin Yvon spectrometer. Depth profiling of the proton-exchanged layer of Y-2 by Ra-spectra was performed by moving the focused laser beam from the substrate to the surface of the layer in approximately 0.5 μm steps.

Table 1. Technological and waveguide parameters of the proton-exchanged waveguides (T – vapor temperature, t – duration of the PE-process, M- number of waveguide modes at $\lambda = 0.633 \mu\text{m}$, Δn_e – the extraordinary refractive index change, d – the waveguide depth).

Sample	Proton Source	T ($^{\circ}\text{C}$)	t (h)	M	Δn_e	d (μm)	Losses (dB/cm)	Phase composition (spectroscopic evidences)		
								Mode	IR	Ra
Z-1	LiHSO_4 (vapors)	250	3.50	6	0.1491	2.66	Table 2	$\beta_1, \beta_3, \beta_4$	$\alpha, \beta_1, \beta_3, \beta_4$	α, β_i, β_4
NMZ-1	NH_4HSO_4 (melt)	230	3.33	9	0.1508	2.47	Table 2	$\beta_1, \beta_3, \beta_4$	$\alpha, \beta_1, \beta_3, \beta_4$	α, β_i, β_4
NMZ-5	LiHSO_4 (melt)	175	1.50	1	0.1222	0.62	~10	β_1, β_3	α, β_1, β_3	α, β_i
X-3	LiHSO_4 (vapors)	160	4.00	1	0.0162	0.52	~10	β_1, β_3	α, β_1, β_3	α, β_i
Y-2	$\text{C}_6\text{H}_5\text{COOH} + 0.5\% \text{C}_6\text{H}_5\text{COOLi}$	230	3.00	3	0.1134	1.56	Table 2	$\beta_1, k_1/k_2$	$\alpha, \beta_1, k_1/k_2$	$\alpha, \beta_1, k_1/k_2$

Table 2. Mode distribution of the optical losses for the multimode waveguides (m - mode number).

Sample	Z-1	NMZ-1	Y-2
Optical Losses (dB/cm)	1-2 (m=0) 6-7 (m=3)	1-2 (m=0,1,2)	0.7-0.8 (m=0)
	3-4 (m=1) ~10 (m=4)	4-5 (m=3,4,5,8)	4-5 (m=1)
	5-6 (m=2) ~10 (m=5)	1-2 (m=6,7)	~ 10 (m=2)

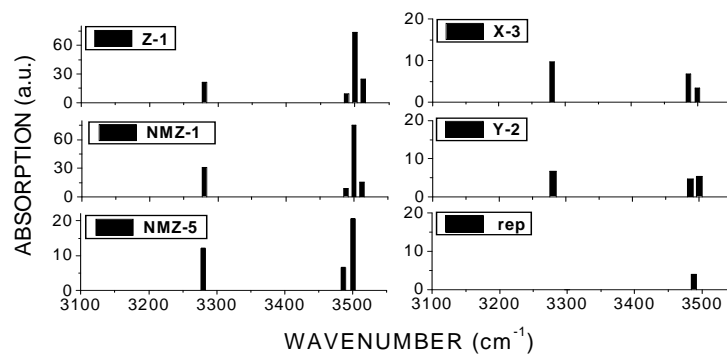


Fig. 1. Infrared spectra deconvolution: schematic presentation of the frequency positions and integrated intensities of the components.

3. Discussion

The value of the extraordinary refractive index change $\Delta n_e = 0.15$ for Z-1 and ZNM-1, and its gradual change to 0.12 on the optical profiles of the waveguides [3], lead to the suggestion [2] that these waveguides contain the β_4 -phase, which is characterized by a higher level of proton doping for monocrystalline $\text{H}_x\text{Li}_{1-x}\text{NbO}_3$ ($0.65 \leq x \leq 0.7$) [2]. The β_4 -phase can exist only in Z-cut proton exchanged lithium niobate, and only together with the β_3 - and β_1 -phases of lower values of x: $0.53 \leq x \leq 0.65$ for the β_3 -phase and $0.44 \leq x \leq 0.52$ for the β_1 -phase [2]. Thus, the waveguides Z-1

and NMZ-1 consist of at least three β_i -phases: β_1 , β_3 and β_4 . The third waveguide – NMZ-5 – was single-mode. It should be in the β_1 , $\beta_1+\beta_2$ or $\beta_1+\beta_3+\beta_4$ phase, since the value of Δn_e exceeds 0.12, indicating that a β_i -phase or phases have been formed during the PE-process [2].

The same considerations applied to X- and Y-cut samples lead to the conclusion that X-3 contains the β_3 -phase [2], which can be found only together with the β_1 -phase. The optical parameters of Y-2 correspond to the coexistence of the β_1 and k_1/k_2 phases.

As shown in Tables 1 and 2, most waveguide modes have high optical losses confirming the presence of more than one crystalline phase in the PE-layer: The interfaces of the phase sublayers cause losses when crossed by the propagating mode. This is why in the cases of multimode waveguides, the losses are different for each propagating mode. A single-mode waveguide having a multiphase structure should have the highest losses, since the propagating mode crosses all interfaces of the sublayers formed by different phases. Indeed, the losses in NMZ-5 and X-3 are really the highest.

Looking at the IR-spectra deconvoluted in Fig. 1, we can see that most of the spectra consist of a strong peak at about 3500 cm⁻¹, polarized perpendicularly to the Z-axis and attributed to the β_1 -phase, and a broad unpolarized band peaked at about 3250-3280 cm⁻¹, attributed to the β_2 , β_3 and β_4 phases [2]. The OH-spectrum of the bulk (reper) exhibits a polarized band centered at 3488 cm⁻¹. This peak is attributed to the α -phase H_xLi_{1-x}NbO₃ (0 ≤ x ≤ 0.12) [2]. The OH-absorption band was fitted to these three components. For the strongly protonated samples NMZ-1 and Z-1, a fourth additional component begins to appear at about 3512 cm⁻¹. This band could be attributed to the β_4 -phase that exists only in these two waveguides. For X-3 and Y-2 samples, an unpolarized shoulder at 3250 cm⁻¹ confirms the presence of β_2 - or β_3 - phases in the X-cut sample, or k_1/k_2 phases in the Y-cut sample. In all cases, the decomposition shows that the area of the α -phase band increase after PE, and thus the α -phase has to be added to the phase composition of all layers obtained in the present experiments. Since this phase is situated between the substrate and the higher proton-exchanged layers in some cases (a thin layer of the β_1 -phase over the α -phase, for example), it makes the transition of the layer, strained by proton exchange, to the substrate more gradual, preventing high losses at their interface. Since the component due to the substrate α -phase was extracted from the spectra after deconvolution, only the components of the layers' spectra are present in the histograms.

In the Raman scattering geometries used, the phonon spectrum of pure LiNbO₃ consists of four A1(TO)-phonons (at 254, 275, 332 and 632 cm⁻¹), polarized along the Z-axis, and seven E(TO)-phonons (at 152, 236, 263, 332, 370, 431 and 578 cm⁻¹), polarized along the X- or Y-axis [7]. Fig. 2 shows that the main changes introduced by PE concern the intensity of the main spectral lines, the appearance of new ones and the spectra intensity attenuation compared to those of the surface. The strong attenuation occurs in samples with the maximal degree of disorder [8]. According to [9] the most notable changes after PE are in the band intensities in the 200-500 cm⁻¹ region and, most importantly, the appearance of a broad band in the 650-750 cm⁻¹ is observed. This originates from a paraelectric-like phase, as well as the A1(TO)-peak at 690 cm⁻¹ [10]. For our samples, we can see this peak even in the E(TO) spectra. As is known, in a strained crystal some coupling between the E(TO) and A1(TO) modes is possible. Thus, we could consider the presence of such a large band as evidence for the existence of phases having the highest value of x, as β_4 for the Z-cut samples (Z-1, NMZ-1) or β_1 for the Y-cut sample. The new band present in all spectra of our PE-layers could be due to second-order Raman scattering [11] which is a combined Ra-scattering from coexisting ferroelectric (α) and paraelectric (β_i) LiNbO₃. Hence, the Ra-spectra give some evidence for the presence of an α -phase in the PE layer, as the IR-absorption spectra also do (Fig. 1). The set of narrow peaks in the Ra-spectra also indicates a high value of x and the presence of β_i -phases (i=1-3) [12]. Since all spectra have such sets of peaks, we could conclude that the layers include some β_i -phases, β_1 and β_3 being indistinguishable from a spectroscopic point of view. The peak appearing at 878 cm⁻¹ (Fig.2-b, c, d) comes from the E(LO)-mode, excited due to the strained lattice, and also confirms the high level of H⁺-doping.

The depth profiling of Y-2 (Fig. 2-f) shows some intensity transfer between the A1(TO)-mode at 690 cm⁻¹ and the E(TO)-mode at 630 cm⁻¹, which are excited in the same geometry because of the crystal lattice perturbation introduced by PE. The changes of the E(TO) Ra-spectra originate from the internal strains in the sample as a result of order-disorder distribution of protons, whereas the changes of the A1(TO) Ra-spectra are due to the displacement of the positive and negative ions [12]. Thus, in strongly protonated samples, the E(TO) intensities have to be stronger and at the same time the A1(TO) intensities have to be weaker. Since the intensity of the 690 cm⁻¹ band (A1) increases toward the substrate, and that at 630 cm⁻¹ (E) decreases, we could conclude that the layer

contains sub-layers, having different values of x (decreasing towards the substrate), i.e. presenting different phases in addition to the α - and β_1 -phase, as commented upon above. They should be k_1/k_2 phases, which are also indistinguishable spectroscopically.

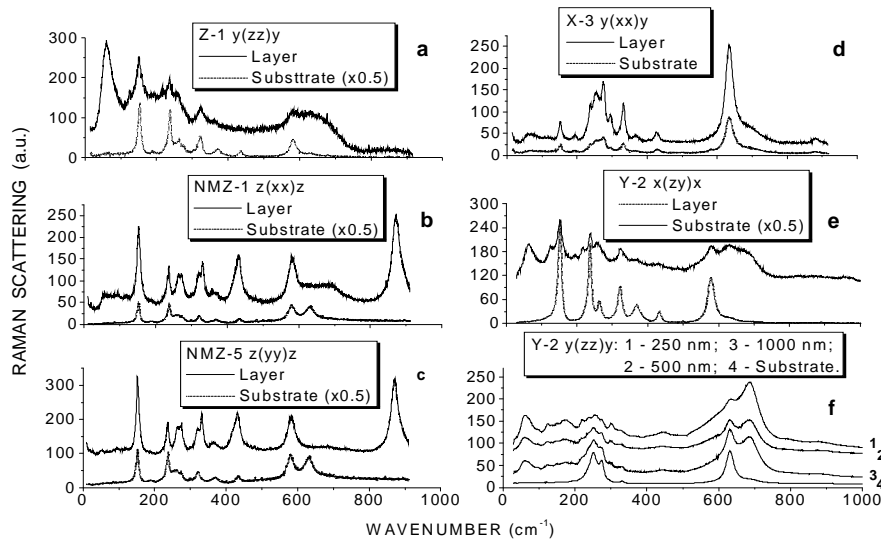


Fig. 2. Ra-spectra (A1(TO) and E(TO) modes) of the samples investigated (a-e). Micro-Raman depth profiling of the sample LY-2 (f).

4. Conclusions

The phase content of PE-waveguides in Z-cut LiNbO₃ was studied by using waveguide-spectroscopy together with IR-absorption and Raman spectroscopy. The combined analysis allows identification of phases in the waveguide layer of multiphase waveguides. It can be used for adjustment of fabrication conditions for obtaining defined phase contents needed for waveguide devices with improved stability and characteristics.

The investigation performed is a logical continuation of the work [3,4] concerning the investigation of new proton sources and technological conditions for producing waveguides by proton exchange in LiNbO₃ and LiTaO₃.

References

- [1] J. L. Jackel, C. E. Rice, J. J. Veselka, *Appl. Phys. Lett.* **41**, 607 (1982).
- [2] Yu. N. Korkishko, V. A. Fedorov, *IEEE J. Select. Top. Quant. El.*, **2**, 1 (1996).
- [3] M. Kuneva, S. Tonchev, M. Sendova-Vasileva, D. Dimova-Malinovska, P. Atanasov, *Sensors and Actuators A* **99**, 154 (2002).
- [4] M. Kuneva, S. Tonchev, P. Dimitrova, *J. Mater. Sci.: Mater. in Electronics*. **14**, 859 (2003).
- [5] J. M. White, P. E. Heidrich, *Appl. Opt.* **15**, 151 (1976).
- [6] R. Ulrich, *J. Opt. Soc. Am.* **60**, 1337 (1970).
- [7] X. Yang, G. Lan, B. Li, H. Wang, *phys. stat. sol. (b)* **141**, 287 (1987).
- [8] X. Wu, M.-S. Zhang, D. Feng, *Appl. Phys. Lett.* **65**, 2916 (1994).
- [9] G. R. Paz-Pujalt, D. D. Tuschel, *Appl. Phys. Lett.* **62**, 3411 (1993).
- [10] Yu. Voron'ko, A. Kudryavtsev, V. Osiko, A. Sobo, E. Sorokin, *Sov. Phys. Solid State* **29**, 771 (1987).
- [11] R. Claus, G. Borstel, E. Wiesendanger, L. Stefan, *Z. Naturf.* **27a**, 1187 (1972).
- [12] X.-L. Wu, M.-S. Zhang, D. Feng, *phys. stat. sol. (a)* **153**, 233 (1996).